*Published online 9 April 2009*

*Nucleic Acids Research, 2009, Vol. 37, No. 9* ***e70***
*doi:10.1093/nar/gkp211*

# Accurate characterization of weak macromolecular interactions by titration of NMR residual dipolar couplings: application to the CD2AP SH3-C:ubiquitin complex

**Jose Luis Ortega-Roldan[1], Malene Ringkjøbing Jensen[2,*], Bernhard Brutscher[3], Ana I. Azuaga[1], Martin Blackledge[2,*] and Nico A. J. van Nuland[1,4]**

[1]Departamento de Química Física e Instituto de Biotecnología, Facultad de Ciencias, Universidad de Granada, Fuentenueva s/n, 18071 Granada, Spain, [2]Protein Dynamics and Flexibility by NMR, Institut de Biologie Structurale Jean-Pierre Ebel, CEA; CNRS; UJF UMR 5075, 41 Rue Jules Horowitz, Grenoble 38027, France, [3]Laboratoire de RMN, Institut de Biologie Structurale Jean-Pierre Ebel, CEA; CNRS; UJF UMR 5075, 41 Rue Jules Horowitz, Grenoble 38027, France and [4]Structural Biology Brussels, VIB Department of Molecular and Cellular Interactions, Vrije Universiteit Brussel, Pleinlaan 2, 1050 Brussel, Belgium

Received February 10, 2009; Revised March 13, 2009; Accepted March 16, 2009

## ABSTRACT

**The description of the interactome represents one of key challenges remaining for structural biology. Physiologically important weak interactions, with dissociation constants above 100 μM, are remarkably common, but remain beyond the reach of most of structural biology. NMR spectroscopy, and in particular, residual dipolar couplings (RDCs) provide crucial conformational constraints on intermolecular orientation in molecular complexes, but the combination of free and bound contributions to the measured RDC seriously complicates their exploitation for weakly interacting partners. We develop a robust approach for the determination of weak complexes based on: (i) differential isotopic labeling of the partner proteins facilitating RDC measurement in both partners; (ii) measurement of RDC changes upon titration into different equilibrium mixtures of partially aligned free and complex forms of the proteins; (iii) novel analytical approaches to determine the effective alignment in all equilibrium mixtures; and (iv) extraction of precise RDCs for bound forms of both partner proteins. The approach is demonstrated for the determination of the three-dimensional structure of the weakly interacting CD2AP SH3-C:Ubiquitin complex ($K_d = 132 \pm 13$ μM) and is shown, using cross-validation, to be highly precise. We expect this methodology to extend the remarkable and unique ability of NMR to study weak protein–protein complexes.**

## INTRODUCTION

Following the successful development of structural genomic initiatives dedicated to the determination of the three-dimensional conformation of a large number of proteins (1,2), attention is now turning to the characterization of the multitude of interactions between these proteins that control cellular processes and biological function (3–6). This paradigm, the description of the molecular basis of the interactome, is expected to provide a comprehensive portrayal of the overall interaction structure of an organism's proteome, thereby representing one of the major challenges for structural biology in the coming decade (7). Although very weak protein–protein interactions (dissociation constant $K_d > 10^{-4}$ M) are expected to be important for a vast range of cellular events, such as transcription and replication, signal transduction, transient formation of encounter complexes and assembly of protein complexes, they remain the least well characterized (8).

NMR is one of the most powerful tools for the study of biomolecular complexes due to its sensitivity to protein–protein interactions with equilibrium dissociation constants varying over many orders of magnitude, including weak encounter complexes that can barely be detected using other biophysical techniques (8–10). In addition to the mapping of chemical shift (CS) changes induced by the proximity of the partner protein, cross-relaxation

*To whom correspondence should be addressed. Tel: +33 438789554; Fax: +33 438785494; Email: martin.blackledge@ibs.fr
Correspondence may also be addressed to Malene Ringkjøbing Jensen. Email: malene.ringkjobing-jensen@ibs.fr

(nOe)-derived intermolecular distance restraints and paramagnetic relaxation enhancements (9), residual dipolar couplings (RDCs) (11,12) have been shown to provide highly complementary orientational information that can be crucial for the determination of an accurate conformation of the complex (13–21). In the case of weak protein–protein complexes, where orientational constraints can be the most critical due to the insensitivity of NOESY experiments, the use of RDCs is seriously compromised by numerous experimental and theoretical complications. This is essentially because under conditions where the complex is too weak to be isolated experimentally, measured RDCs report on both bound and free forms of the molecule. Alignment characteristics of free and bound forms of both proteins must therefore be determined and alignment levels accurately calibrated.

In this work, we address these problems and present a generally applicable protocol for the measurement, analysis, and interpretation of RDCs for the refinement of the structure of weak protein–protein complexes. The protocol includes differential isotopic labeling of the two proteins (22) to allow the simultaneous measurement of RDCs at different molar ratios of both partners, and uses a robust linear extrapolation approach to determine the bound form RDCs from partner proteins in the same experimental mixtures. The protocol is shown via entirely independent cross-validation of data not used in the analysis to be highly accurate, and the importance of this methodology is clearly demonstrated by a detailed analysis of the significant structural errors that can be induced when residual components from the free forms of either protein contribute to the measured RDCs.

We apply this approach to the study of the complex formed between SH3-C, the third SH3 domain of CD2AP (CD2-associated protein) and ubiquitin. Ubiquitin is known to regulate a wide variety of cellular activities ranging from transcriptional regulation to cell signaling and membrane trafficking (23,24). Many cellular activities of ubiquitin are mediated by mono- rather than poly-ubiquitin, and its functions are deciphered by various ubiquitin-binding proteins. Similar to ubiquitin-binding domains, SH3 domains are found in proteins with different biological functions. SH3 domains form a highly conserved family of domains, but their amino acid composition varies at a few key sites, allowing for a wide range of molecular targets. Recently, it was found that a subset of SH3 domains constitutes a new, distinct type of ubiquitin-binding domains (25). The structure of the complex between Sla1 SH3-3 and ubiquitin shows that the ubiquitin-binding surface of the Sla1 SH3 domain overlaps largely with the canonical binding surface for proline-rich ligands and that like many other ubiquitin-binding motifs, the SH3 domain engages the Ile44 hydrophobic patch of ubiquitin (26). Here, we use NMR chemical shift perturbation and bound form RDCs for both proteins extrapolated from specifically developed RDC titration experiments, to determine a structural model of the CD2AP SH3-C:Ubiquitin complex.

## THEORETICAL ASPECTS

Residual dipolar couplings report on the orientation of internuclear vectors connecting two nuclei $i$ and $j$ with respect to the alignment tensor of a rigid molecule as follows:

$$D_{ij} = -\frac{\gamma_i \gamma_j \mu_0 h}{16\pi^3 r_{ij}^3}\left[A_a(3\cos^2\theta - 1) + \frac{3}{2}A_r \sin^2\theta\cos(2\varphi)\right] \quad \mathbf{1}$$

$A_a$ and $A_r$ are the axial and rhombic components of the alignment tensors, and $\theta$, $\varphi$ define the orientation of the internuclear vector with respect to the alignment tensor and $r_{ij}$ is the internuclear distance. However, in the case of weak binding and fast exchange between free and bound forms of the proteins, experimental couplings, $D_{ij}^{\text{exp}}$, report on a combination of couplings in bound and free forms of the molecule ($D_{ij}^{\text{bound}}$ and $D_{ij}^{\text{free}}$):

$$D_{ij}^{\text{exp}} = p_{\text{bound}} D_{ij}^{\text{bound}} + (1 - p_{\text{bound}}) D_{ij}^{\text{free}} \quad \mathbf{2}$$

where $p_{\text{bound}}$ is the fraction of the protein in the bound state. In theory, assuming that the ratio of bound and free forms of the proteins is known, $D_{ij}^{\text{bound}}$ can be determined using Equation (2) from precise measurements of $D_{ij}^{\text{exp}}$ and $D_{ij}^{\text{free}}$. Such a procedure has been applied to the study of weakly binding molecules to larger proteins where the nature of the larger system provides *a priori* knowledge allowing a simplification of the problem (18–21). Without knowledge of the structure of the complex the contribution of the measured values emanating from the free and bound forms of the proteins can be very difficult to quantitatively separate.

The use of RDCs to determine the relative orientation of partners in weak protein–protein complexes is also severely compromised by additional experimental and analytical difficulties, including the reproduction of identical absolute alignment conditions for the samples necessary for error-free subtraction of the free-form RDCs, and the associated potential for the propagation of experimental uncertainty that is inherent in the necessary subtraction required to derive values of $D_{ij}^{\text{bound}}$. RDCs from the bound form of the labeled proteins can of course be isolated under conditions where essentially all of these proteins are bound in the complex, but in the case of weak complexes this saturation limit requires potentially prohibitive concentrations of the partner protein.

We therefore propose a procedure that simultaneously determines the alignment characteristics of both free and bound forms of the proteins, and determines the level of alignment in each medium. Instead of measuring a single mixture, RDCs are measured over a range of titration mixtures $m_i$ of free and bound forms of both proteins. In each of the mixtures the measured RDC, $D_{ij}^{m,\text{exp}}$, is given by a slightly modified version of Equation (2):

$$D_{ij}^{m,\text{exp}} = \lambda_m D_{ij}^{m} = \lambda_m\left\{p_{\text{bound}} D_{ij}^{\text{bound}} + (1 - p_{\text{bound}}) D_{ij}^{\text{free}}\right\} \quad \mathbf{3}$$

where $\lambda_m$ is a scaling factor defined by the absolute level of alignment that is in turn determined by the concentration

of the alignment medium, and $p_{\text{bound}}$ spans different values for the two proteins. $D_{ij}^{\text{free}}$ and $D_{ij}^{\text{bound}}$ are given by:

$$D_{ij}^{\text{free}} = -\frac{\gamma_i\gamma_j\mu_0 h}{16\pi^3 r_{ij}^3}\left[A_a^{\text{free}}(3\cos^2\theta^{\text{free}} - 1) + \frac{3}{2}A_r^{\text{free}}\sin^2\theta^{\text{free}}\cos(2\varphi^{\text{free}})\right] \quad \mathbf{4}$$

$$D_{ij}^{\text{bound}} = -\frac{\gamma_i\gamma_j\mu_0 h}{16\pi^3 r_{ij}^3}\left[A_a^{\text{bound}}(3\cos^2\theta^{\text{bound}} - 1) + \frac{3}{2}A_r^{\text{bound}}\sin^2\theta^{\text{bound}}\cos(2\varphi^{\text{bound}})\right] \quad \mathbf{5}$$

$A_a$ and $A_r$ refer to the free or bound alignment tensors, and the two spherical coordinates ($\theta$, $\varphi$) refer to the orientation of the internuclear vector with respect to the alignment tensor in the two forms. Note that this simple linear relationship [Equation (3)] holds irrespective of changes in structure and dynamics of the site of interest in the complex. For some alignment media $\lambda_m$ can be estimated from the deuterium quadrupolar coupling from the $D_2O$ present in the sample. This is not a precise metric however, and it is therefore preferable to exploit the combined dependence of Equation (3) to determine the exact scaling factors, by adjusting $\lambda_m$ to maintain optimal linearity of $D_{ij}^m$ relative to $p_{\text{bound}}$. The same scaling factor is applied to both proteins in the respective mixtures as differential isotope labeling allows simultaneous measurement of RDCs in the two proteins. All couplings from both proteins are used in this procedure ensuring a high level of precision and robustness implicit in this optimization. Following this adjustment the expected values of the bound forms of the RDCs from both proteins are determined from the resulting linear titration relationships established for each individual RDC. This procedure turns out to be highly robust and significantly more accurate than subtraction of a single value scaled on the basis of $^2$D splitting (*vide infra*).

## MATERIALS AND METHODS

### Protein expression and purification

For clarity, we use the residue numbering of CD2AP SH3-C of PDB entry 2JTE throughout the text. Unlabeled, $^{15}$N-labeled and $^{15}$N,$^{13}$C-labeled CD2AP SH3-C was obtained as described (27). Unlabeled and $^{15}$N-labeled ubiquitin were purchased from both Cortecnet and Spectra Stable Isotopes. $^{15}$N/$^{13}$C-labeled ubiquitin was kindly provided by Varian Inc.

Protein concentrations were determined by absorption measurements at 280 nm using an extinction coefficient of 13 980 and 1450 $\text{cm}^{-1}\,\text{M}^{-1}$ for SH3-C and ubiquitin, respectively, determined using the ProtParam algorithm (www.expasy.ch).

### NMR chemical shift perturbation

All NMR titration experiments were performed at 25°C on a Varian NMR Direct-Drive Systems spectrometer ($^1$H frequency of 600.25 MHz) equipped with a triple-resonance PFG-XYZ probe. CD2AP SH3-C and ubiquitin samples were prepared for NMR experiments in 93% $H_2O$/7% $D_2O$, 50 mM NaPi, 1 mM DTT at pH 6.0. The backbone amide and $^{15}$N frequencies of CD2AP SH3-C under the above conditions, previously assigned at pH 2.0 (27), were obtained first by comparing 2D $^{15}$N-HSQC spectra at pH 2.0, 3.0, 6.0 and 7.0 and confirmed by a single HNCACB triple resonance experiment acquired on $^{15}$N,$^{13}$C-labeled CD2AP SH3-C at pH 6.0. An HNCACB triple resonance spectrum was also recorded on a $^{13}$C/$^{15}$N-labeled ubiquitin to confirm backbone assignment at pH 6.0.

The SH3-binding site on ubiquitin was obtained by titrating with increasing amounts of unlabeled CD2AP SH3-C domain into a 0.25 mM $^{15}$N-ubiquitin sample at pH 6.0, 25°C. Similarly, the ubiquitin-binding site on CD2AP SH3-C was obtained by titrating with increasing amounts of unlabeled ubiquitin into a 0.25 mM $^{15}$N-SH3-C sample under the same conditions. The progress of the titrations was monitored by recording one-dimensional $^1$H and two-dimensional $^1$H-$^{15}$N HSQC spectra.

The magnitude of the chemical shift deviations ($\Delta\delta$) was calculated using the equation:

$$\Delta\delta_{\text{ppm}} = \sqrt{(\Delta\delta_{\text{HN}})^2 + \left(\frac{\Delta\delta_N}{6.51}\right)^2} \quad \mathbf{6}$$

where the difference in chemical shift is that between the equilibrium mixture and free forms of the different proteins.

All NMR data were processed using NMRPipe (28) and analyzed by NMRView (29).

### Measurement of RDCs

RDCs were measured in samples partially aligned in a liquid-crystalline medium consisting of a mixture of 5% penta-ethyleneglycol monododecyl ether ($C_{12}E_5$) and hexanol (30). For the $^{13}$C/$^{15}$N-labeled protein (SH3) in the free form or in diverse mixtures of free and complex, a set of four different RDCs ($^1D_{NH}$, $^1D_{C\alpha C'}$, $^2D_{HNC'}$ and $^1D_{C\alpha H\alpha}$) was measured per sample using 3D BEST-type HNCO or HNCOCA experiments (31,32). Coupling constants were obtained from line splittings in the $^{13}$C dimension using the nmrPipe nlinLS fitting routine or using Sparky (33). For the $^{15}$N-labeled protein (ubiquitin) in free or in the complex, $^1D_{NH}$ were measured from a pair of spin-state-selected $^1$H-$^{15}$N correlation spectra recorded using the pulse sequence shown in figure S4. The pulse sequence uses a DIPSAP filter (34) for J-mismatch compensated spin-state selection, and the BEST concept for longitudinal relaxation and sensitivity enhancement (31,32). In addition, signals from the $^{13}$C/$^{15}$N labeled binding partner are removed by additional transfer steps from $^{15}$N to $^{13}$CO. After this transfer step the presence of orthogonal coherences for the spin systems from $^{15}$N-only and $^{13}$C/$^{15}$N-labeled proteins is exploited to suppress the unwanted signals by means of pulsed field gradients and phase cycling. Total measurement time for one titration point is ~1 day.

### RDC refinement of the SH3-C domain of CD2AP in complex with ubiquitin

The program SCULPTOR (35) has recently been developed as an addition to the program CNS (36). The refinement protocol involves a restrained MD calculation using the standard CNS force field. Starting structures were taken from a selection of 10 structures determined using HADDOCK (37) based on ambiguous intermolecular restraints (AIRs). Initial sampling was further increased by including a sampling period of 10 ps at 700 K that allows for the SH3 domain to reorient freely without RDCs or AIR restraints. Following this, both ubiquitin and SH3 conformations are fixed and the alignment tensor is allowed to evolve freely to determine initial estimates from the SH3 structure (38,39) (there are four RDC types available for this structure). Both molecules and tensors are then freed with the initial sampling period at 1000 K for 5 ps during which time both AIRS and RDCs are scaled from 0.1% to 100% of their final values. The backbone conformation of the segment (1–70) of ubiquitin is restrained to its initial coordinates using a harmonic potential, while the experimentally measured nOes from the free form of SH3 are used as restraints. Note that the RDCs measured in the bound form can be used to determine structural changes upon binding, as the RDC titration approach provides accurate constraints for bound forms of both partners irrespective of differences in structure and dynamics between the free and bound forms (see below). AIR restraints are used as described in the supporting information. Sampling of restraints is followed by a 5-ps sampling stage and slow cooling over 5 ps to 100 K and energy minimization. The protocol is repeated 30 times for each starting structure.

## RESULTS AND DISCUSSION

### Chemical shift perturbation of ubiquitin and SH3

NMR chemical shifts of protein residues are highly sensitive to changes in the local environment, and chemical shift perturbations are therefore widely used to map intermolecular interfaces of protein complexes (40) and to drive the docking of two interacting partners in order to obtain a structural model of the complex (41,42). Titrations of $^{15}$N-labeled ubiquitin with increasing amounts of SH3-C domain at 25°C and vice versa caused a selective shift of amide proton and nitrogen resonances of several ubiquitin and SH3-C residues (Figure 1), indicating a specific union between the two proteins. The most significant changes in the chemical shift of the HSQC cross-peaks of the SH3 domain can be observed at the *RT loop* (residues 18–23), the *nSrc loop* (residues 37–39), the beginning of the β-*III strand* (residues 42–44) and residues 54–58. Significant changes in the chemical shift of the HSQC cross-peaks of ubiquitin are mainly observed in two typical binding regions, namely that of Ile44 and of Gly76.

The SH3-Ubiquitin complex is in fast exchange with the free forms of the partners as shown from the chemical shift titration in Figure 1A and B (upper panels). Thus, no significant line broadening of the resonances is observed during the titration. A $K_d$ of $132 \pm 13\,\mu M$ was determined (Figure 1C, D) on the basis of a simultaneous fit of the combined $^1H^N$ and $^{15}N$ shifts of residues 18, 19, 20, 21, 38, and 44 (SH3) to titration of added ubiquitin, and 42, 45, 47, 68 and 73 (Ubiquitin) to titration of added SH3. The affected sites on SH3 are identified from the extent of the chemical shift perturbations upon addition of ubiquitin and vice versa (Figure 1A and B, lower panels), and these sites were transformed into ambiguous intermolecular distance restraints (AIRs, see 'Methods' section in Supplementary Data). The program HADDOCK (37) was used to calculate the structure of the complex on the basis of these restraints. The 200 lowest energy structures were refined in a shell of water, and one representative structure of each of 10 identified clusters were selected (see Supplementary Data, Figure S1) for further refinement of the conformation of the complex using RDCs measured of both proteins in the bound forms.

### Titration of RDCs for ubiquitin and SH3 in the protein–protein complex

SH3 was uniformly isotopically labeled $^{13}$C and $^{15}$N, and ubiquitin was uniformly $^{15}$N labeled. This allowed the use of isotopically filtered RDC measurements (see 'Materials and Methods' section) such that couplings from both partners were measured in three mixtures ($m_1$, $m_2$ and $m_3$) of the two components. $^{15}N$–$^1H^N$ RDCs were measured in ubiquitin and $^{15}N$–$^1H^N$, $^{13}C'$–$^1H^N$, $^{13}C'$–$^{13}C^\alpha$ and $^{13}C^\alpha$–$^1H^\alpha$ were measured for SH3. This labeling scheme was adopted to simplify spectral analysis when RDCs are measured from both partners in the same sample, an integral part of the method developed here (22). These RDCs were also measured in independently aligned free forms of both molecules (samples $m_{0,ubi}$ and $m_{0,sh3}$). For each partially aligned sample, $p_{bound}$ was determined from the ratios of intensities (volumes) of resonances in $^1H$–$^{15}N$ HSQC spectra containing peaks from both SH3 and ubiquitin. The mixtures ($m_1$, $m_2$ and $m_3$) were thus estimated to represent $p_{bound}$ values of (0.44, 0.75 and 0.84) for SH3 and (0.79, 0.61 and 0.49) for ubiquitin.

Correlation plots of $^1D_{NH}$ measured in the free forms of SH3 and ubiquitin compared to values measured at the other three mixtures are indicative of differently oriented alignment tensors in the free and bound forms of both proteins, in particular SH3 (Figure 2 and Table 1). RDCs measured in free forms and mixtures of SH3 and ubiquitin were compared to known structures of the two proteins [pdb codes: 1D3Z (43) for ubiquitin and the RDC refined structure of SH3] using the program MODULE (44). All data sets fit reasonably well to these structures, as illustrated in Figures S2 and S3 in Supplementary Data and Table 1.

In the case of the RDCs emanating from mixtures of $D_{ij}^{bound}$ and $D_{ij}^{free}$, the effective alignment tensor results from a linear combination of the free and bound alignment tensors. The effective tensors resulting from these different combinations can vary significantly in terms of

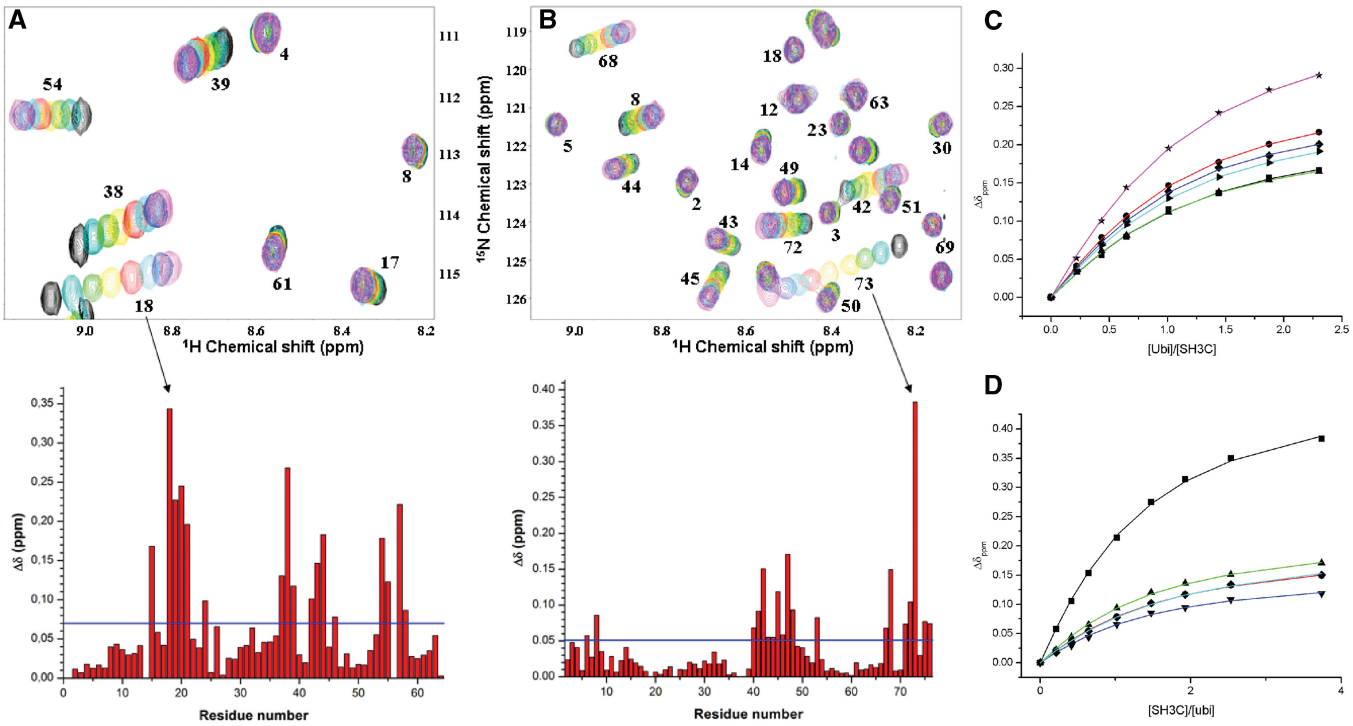


**Figure 1.** Monitoring the binding between ubiquitin and CD2AP SH3-C by NMR chemical shift perturbations. (**A**) $^{1}H$ and $^{15}N$ chemical shift changes upon titrating ubiquitin into a $^{15}N$-labeled CD2AP SH3-C solution. Upper panel: region of $^{1}H$-$^{15}N$ HSQC spectra recorded at increasing amounts of ubiquitin (black to magenta). The chemical shift changes ($\Delta\delta$) between the first and last titration point [Equation (6)] are presented in the bottom panel. (**B**) $^{1}H$ and $^{15}N$ chemical shift changes upon titrating SH3-C into a $^{15}N$-labeled ubiquitin solution. Upper and lower panels as in (A). Blue solid lines indicate the mean chemical shift changes that were used to define the active SH3 and ubiquitin residues used in HADDOCK. (**C**) Changes in chemical shift, $\Delta\delta$, of selected residues in $^{15}N$-labeled SH3 upon addition of unlabeled ubiquitin: black Trp44; red Thr38; green Asp21; blue Glu20; cyan Asn19; magenta Thr18. (**D**) Changes in chemical shift, $\Delta\delta$, of selected residues in $^{15}N$-labeled ubiquitin upon addition of unlabeled CD2AP SH3-C: black Leu73; red His68; green Gly47; blue Phe45; cyan Arg42.

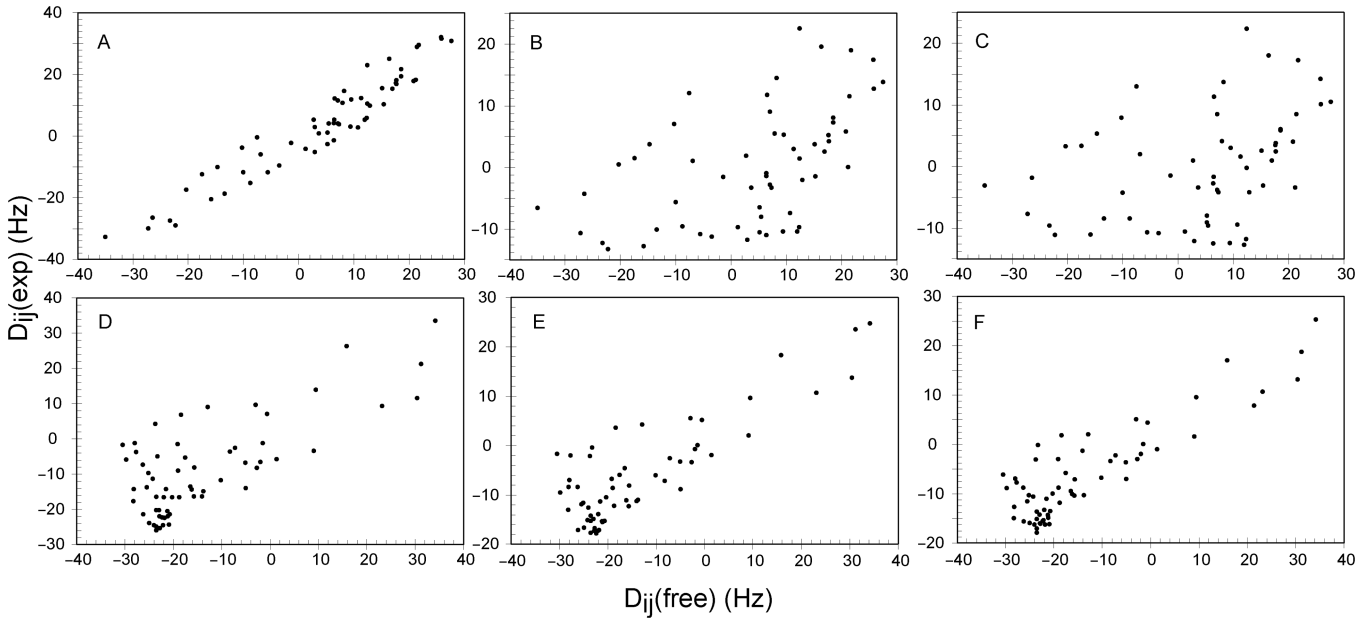


**Figure 2.** Correlation plots of experimental $^{15}N$–$^{1}H^{N}$ RDC data sets. (**A–C**) RDCs in the free form of SH3 versus the RDCs in mixture $m_1$ (A), $m_2$ (B) and $m_3$ (C). (**D–F**) RDCs in the free form of ubiquitin versus RDCs in mixture $m_1$ (D), $m_2$ (E) and $m_3$ (F).

**Table 1.** Alignment tensors of different experimental mixtures

| | Free[a] Ubi | $m_3$ | $m_2$ | $m_1$ | Bound[b] Ubi | Bound[c] Ubi ref | SH3/Ubi[d] ref | Bound[e] SH3 ref | Bound[f] SH3 | $m_3$ | $m_2$ | $m_1$ | Free[g] SH3 |
|---|---|---|---|---|---|---|---|---|---|---|---|---|---|
| $A_a$ ($10^{-4}$) | 12.0 | 12.2 | 12.6 | 13.2 | 13.3 | 13.7 ± 0.2 | 12.9 ± 0.1 | 12.4 ± 0.1 | 11.8 | 10.0 | 10.0 | –14.7 | –25.3 |
| $A_r$ ($10^{-4}$) | 1.10 | 2.1 | 2.4 | 4.5 | 4.5 | 4.3 ± 0.1 | 3.7 ± 0.1 | 3.0 ± 0.1 | 3.0 | 0.3 | 1.2 | –6.7 | –7.3 |
| α (°) | 124 | –24 | –29 | –37 | –40 | – | – | – | –126 | –126 | –144 | –82 | –107 |
| β (°) | 148 | 38 | 39 | 45 | 47 | – | – | – | 54 | 116 | 108 | 150 | 148 |
| γ (°) | 173 | 7.4 | 10 | 20 | 22 | – | – | – | 87 | –99 | –104 | –5 | –28 |

[a]Tensor eigenvalues (scaled by appropriate λ value) resulting from fit of experimental RDCs measured from free Ubiquitin to the structure 1d3z.
[b]Tensor eigenvalues resulting from fit of fully bound Ubiquitin RDCs.
[c]Simultaneous refinement of the structure of 1d3z and alignment tensor eigenvalues using RDCs from fully bound Ubiquitin.
[d]Simultaneous refinement of the complex structure of ubiquitin/SH3 complex using RDCs from fully bound forms of Ubiquitin and SH3.
[e]Simultaneous refinement of the structure of SH3 and alignment tensor eigenvalues using RDCs from fully bound form of SH3.
[f]Fit of experimental RDCs from bound form of SH3 to RDC-refined structure of free-form SH3.
[g]Simultaneous refinement of SH3 (pdb code 2JTE) and alignment tensor eigenvalues using RDCs from SH3 alone.

rhombicity and orientation (simulated data shown in Table S2 in Supplementary Data). It is important to note that the fit of the known structure to the RDCs from any mixture will be equally good, so that the presence of a contribution from the unbound form cannot be identified on the basis of the data reproduction, but as we will see below, these effects can strongly influence the final conformation of the complex. It is therefore important to accurately estimate the true values of the bound RDCs. The procedures we have developed to achieve this are presented in the 'Theoretical aspects' section above and the results described below.

### Extraction of bound form RDCs for ubiquitin and SH3

A total of 1168 experimentally measured RDCs are used to determine the four global scaling parameters $\lambda_i$ and the bound-form values of *both* proteins are extrapolated from the linear build-up for each individual RDC. This approach involves fixing the scaling factor ($\lambda_3$) for one of the three mixtures ($m_3$) of measured couplings, while RDCs from the remaining mixtures are used to simultaneously determine optimal values for $\lambda_1$, $\lambda_2$, $\lambda_{0,ubi}$ and $\lambda_{0,sh3}$. The scaling factors are applied to data measured on both proteins simultaneously such that while $\lambda_1$ corresponds to the required scaling for the equilibrium with majority free form of SH3, it also corresponds to the required scaling for the equilibrium with majority of bound form ubiquitin. This adjustment is independent of which scaling factor is initially fixed. Comparison of the optimal scaling parameters extracted using this approach with the ratio of the overall alignment as estimated from the $^2$H splitting indicates very good similarity between the independently estimated values (Table 2). The approach can therefore be applied with confidence for alignment media or experimental conditions for which the $^2$H splitting does not reflect a linear measure of the effective protein alignment. We note that in cases where the level of alignment is accurately known, an analogous procedure can be applied to adjust the molar ratio of the components for each mixture.

Figure 3 shows the dependence of arbitrarily selected couplings on $p_{bound}$ for both SH3 and ubiquitin after optimization of $\lambda_1$, $\lambda_2$, $\lambda_{0,ubi}$ and $\lambda_{0,sh3}$ relative to $\lambda_3$. Linearity of RDCs with respect to $p_{bound}$ is very clearly observed throughout the molecule. This linearity is expected to exist irrespective of the local structure and dynamics experienced in the two forms, as long as the exchange can be described in terms of a two-state system and that it is fast on the chemical shift and dipolar coupling time scale. To further demonstrate the available precision of this analysis, one-tenth of all RDCs were randomly removed from the total data set and retained for comparison with predicted values derived from the remaining RDCs. Comparisons of experimental and predicted data agree within experimental error for all RDCs (Figure 4). This figure also illustrates the relative precision of the different coupling types relative to their experimental range, with slightly higher dispersion for the smaller $^{13}C'$–$^1H^N$ and $^{13}C'$–$^{13}C^\alpha$ couplings. This analysis can be used to estimate the precision of the extrapolated bound-form couplings in the range of 0.5–1.0 Hz, that combines all contributions to uncertainty, including sample preparation, experimental uncertainty, analytical extraction of the RDCs and extrapolation of the bound-form values and estimation of the fraction of free and bound forms.

**Table 2.** Comparison of $D_2O$ scaling parameters with those extracted from fits

| Sample | $m_1$ | $m_2$ | $m_3$ | $m_{0,sh3}$ | $m_{0,ubi}$ |
|---|---|---|---|---|---|
| Concentration of SH3 (mM) | 0.90 | 0.83 | 0.78 | 1.00 | 0.00 |
| Concentration of ubiquitin (mM) | 0.50 | 1.03 | 1.33 | 0.00 | 0.50 |
| $p_{bound}$ for SH3 | 0.44 | 0.75 | 0.84 | 0.00 | – |
| $p_{bound}$ for ubiquitin | 0.79 | 0.61 | 0.49 | – | 0.00 |
| Experimental $D_2O$ splittings (Hz)[a] | 29 (1.16) | 25 (1.00) | 25 (≡1) | 18 (0.72) | 37 (1.48) |
| $\lambda_m$ | 1.233 | 1.027 | ≡1 | 0.643 | 1.643 |

[a]Number in parentheses indicates the scaled splitting relative to $m_3$ mixture, for comparison with $\lambda_m$ values scaled to $\lambda_3$.

### Refinement of the complex using bound form RDCs for ubiquitin and SH3

Following this procedure, the eigenvalues of the alignment tensors of the scaled free and bound forms represent expected values for a common level of alignment for the

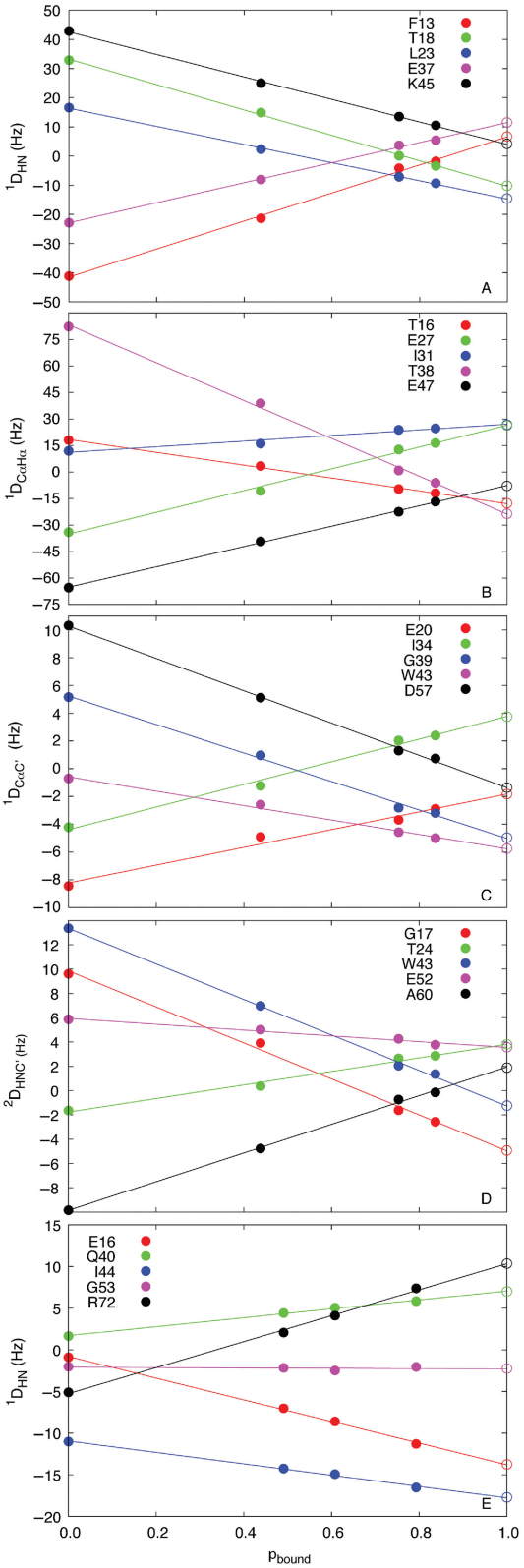


**Figure 3.** Plots of linearly changing RDCs with respect to population of the bound state (*x*-axis). The fully bound values (open circles) represent the values determined by optimization of Equation (3). The remaining values are experimental values, adjusted by optimizing the linearity of the slope by scaling the four parameters $\lambda_1$, $\lambda_2$, $\lambda_{0,ubi}$ and $\lambda_{0,sh3}$ relative to $\lambda_3$. Five sites are shown for each RDC type [(**A–D**) SH3, E Ubiquitin). The selected sites show fits of average quality.

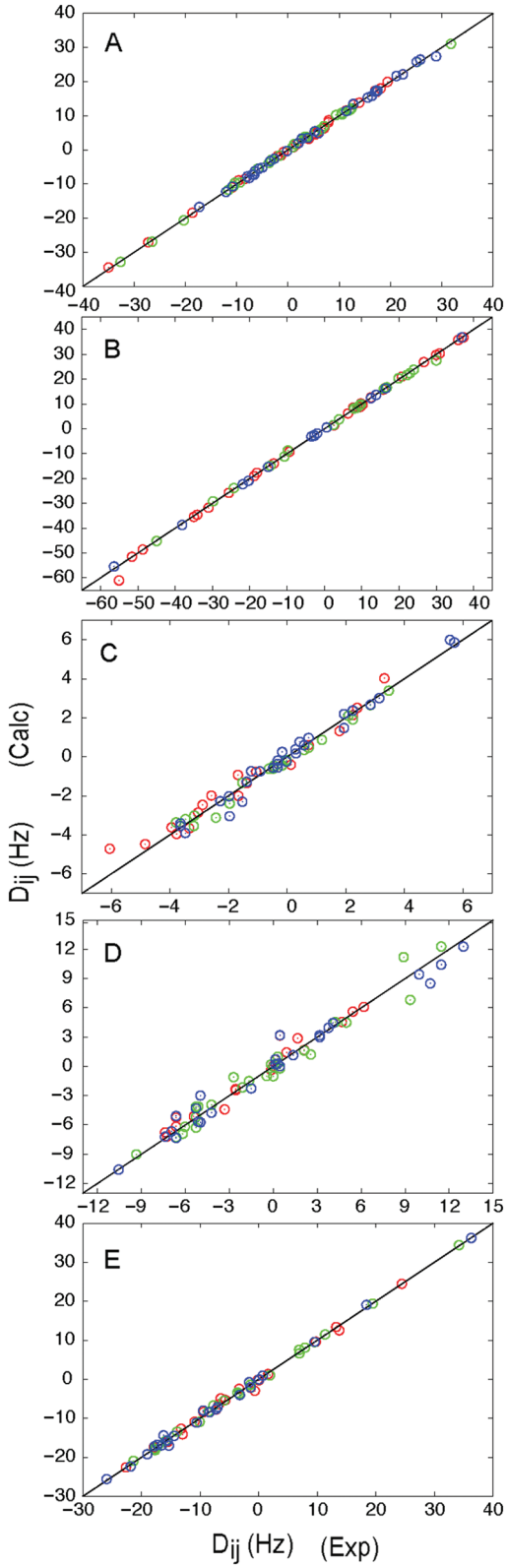


**Figure 4.** Cross-validation of RDC titration analysis. (**A–E**) Back-calculated points from linear fitting approach shown in Figure 3. A total of 120 different RDCs were removed from the analysis, back-calculated (*y*-axis) and compared to the experimental value (*x*-axis). The results of three such calculations are shown in each case (each color represents one of the three analyses) (A) SH3 $^{15}N$-$^1H^N$ RDCs, B – SH3 $^{13}C^\alpha$-$^1H^\alpha$ RDCs, C – SH3 $^{13}C'$-$^{13}C^\alpha$ RDCs, D – SH3 $^{13}C'$-$^1H^N$ RDCs, E- Ubiquitin $^{15}N$-$^1H^N$ RDCs.

two proteins. Comparison of the extrapolated bound form RDCs (open circles in Figure 3) with known structures of the free form proteins (Table 1) shows that the optimal bound form tensor eigenvalues are slightly smaller for SH3 than for Ubiquitin ($A_a \approx 13.3 \times 10^{-4}$, $A_r \approx 4.5 \times 10^{-4}$, compared to $11.8 \times 10^{-4}$ and $3.8 \times 10^{-4}$). This comparison may be biased by a dependence both on angular sampling of RDC-relevant vectors in the two proteins and on the quality of the structures used to determine the tensors (45,46) (a high-resolution RDC-refined structure of ubiquitin—1D3Z and the free form structure of SH3 refined with the four types of RDCs measured on the aligned free form). We therefore carried out a control calculation, wherein the two structures were refined against independent tensors. This leads to optimal tensors for the two refined protein structures of $A_a = 13.7 \times 10^{-4}$, $A_r = 4.3 \times 10^{-4}$ for ubiquitin and $A_a = 12.4 \times 10^{-4}$, $A_r = 3.0 \times 10^{-4}$ for SH3 (Table 1). The apparent differences in eigenvalues of both refined structures are therefore small, and we now focus on the determination of the average orientation of the two proteins in the complex.

Bound-form RDCs determined in this way for both proteins were introduced into a structure refinement procedure starting from conformers from different clusters sampled by HADDOCK using only chemical shift perturbation as intermolecular restraint. The refinement was carried out using the program Sculptor, recently interfaced into CNS, using a refinement protocol assuming a common alignment tensor for both domains whose components are simultaneously determined during the structure refinement (see 'Methods' section in Supplementary Data). The structures with the lowest target function (combining RDC, AIR and nOe violations) in the ensemble are shown in Figure 5A and statistical analysis summarized in Table S3.

The resulting structure of the complex is importantly different from the Sla1 SH3-3:Ubiquitin, (25,26) and the CIN85 SH3-C:Ubiquitin structure (47). A key affinity and specificity determinant for ubiquitin binding was appointed to Phe409 of Sla1, located at the heart of the hydrophobic interface in the SH3–ubiquitin complex. Other SH3 domains with a tyrosine at this position were found to be incompetent to bind ubiquitin (25). Moreover, the Phe409 to Tyr mutation in Sla1 was shown to abolish ubiquitin binding confirming the key role of the phenylalanine residue at this position (25). In our structure, the corresponding phenylalanine residue in the CD2AP SH3-C:Ubiquitin complex is placed at the edge of the binding interface (Figure 5B). In contrast to Sla1 SH3-3, the replacement of this phenylalanine in CD2AP SH3-C by a tyrosine does not abolish ubiquitin binding as monitored by fluorescence, ITC and NMR experiments (data not shown), thus confirming the correctness of our model and indicating that in this case the phenylalanine does not play a key role for the affinity and specificity of ubiquitin binding. The intriguing question that remains is which residues and/or which region of a particular ubiquitin-binding SH3 domain determines the mode/orientation of binding to ubiquitin and whether this difference in binding mode is somehow related to a difference in function. Further progress in this direction will require a more detailed structural and functional study of these complexes, but we note that the recent observation of alternative binding modes present in the formation of this complex already provides evidence for transient encounter complexes that are sampled during the course of this interaction (48).

### Comparison to a determination of RDCs from weak complexes with standard protocols

The true values of the bound form RDCs are not known *a priori*, precluding direct assessment of the relative accuracy of this approach compared to a classical extrapolation from a single mixture. Nevertheless we are able to compare experimentally measured values from one of the mixtures. All $^{15}N$–$^{1}H^{N}$ RDCs measured in SH3 were therefore removed from mixture $m_3$, the analysis was repeated and experimental and predicted values were compared (Figure S6B in Supplementary Data). We have compared this analysis to a prediction of SH3 RDCs from mixture $m_3$ on the basis of values measured in $m_0$ and $m_1$ using a standard extrapolation: $D_{ij}^{m_3} = (\lambda_1 p_3 D_{ij}^{m_1} - \lambda_{0,sh3}(p_3 - -p_1)D_{ij}^{\text{free}})/\lambda_3 p_1$. The populations $p$ are assumed to be accurately known in both cases and in this case the scaling terms $\lambda$ represent the experimentally measured $D_2O$ splitting (Table 2). This case is equivalent to a single mixture where over 50% of SH3 molecules are in the complex. As shown in Figure S6, the ability to reproduce experimental RDCs is significantly improved using the RDC titration approach. The two-point approach, that is directly analogous to standard extrapolation methods based on measurement of a single mixture, suffers from two drawbacks: the combination of experimental errors of the two experimental points that results in random fluctuations of the predicted RDCs and the uncertainty in the actual alignment level that scales all couplings by an unknown systematic error. The combination of these errors results in a poor reproduction of experimental data, and indicates that this kind of approach is likely to provide highly inaccurate RDCs for refinement of molecular orientation. Neither of these sources of error can be corrected without further measurements, and both sources are minimized and at least partially corrected in the RDC titration approach. The possible consequences of these errors in terms of molecular structure are discussed below.

### Refinement against RDCs measured in nonsaturated conditions

The real importance of determining accurate alignment tensors for the precise determination of weakly interacting proteins is illustrated in Figure 6, where data were simulated from the experimentally determined alignment tensors of free and complexed SH3 and Ubiquitin, and used as restraints to orient the partner proteins. Three conditions of incomplete saturation were simulated: 90% saturation for both proteins, 80% saturation and 70% saturation. In each case, the remainder of the protein was assumed to be in its free form. The optimal configurations of the complexes, determined after orientation of the partner proteins such that their effective alignment tensor axes were coaxial and intermolecular contacts

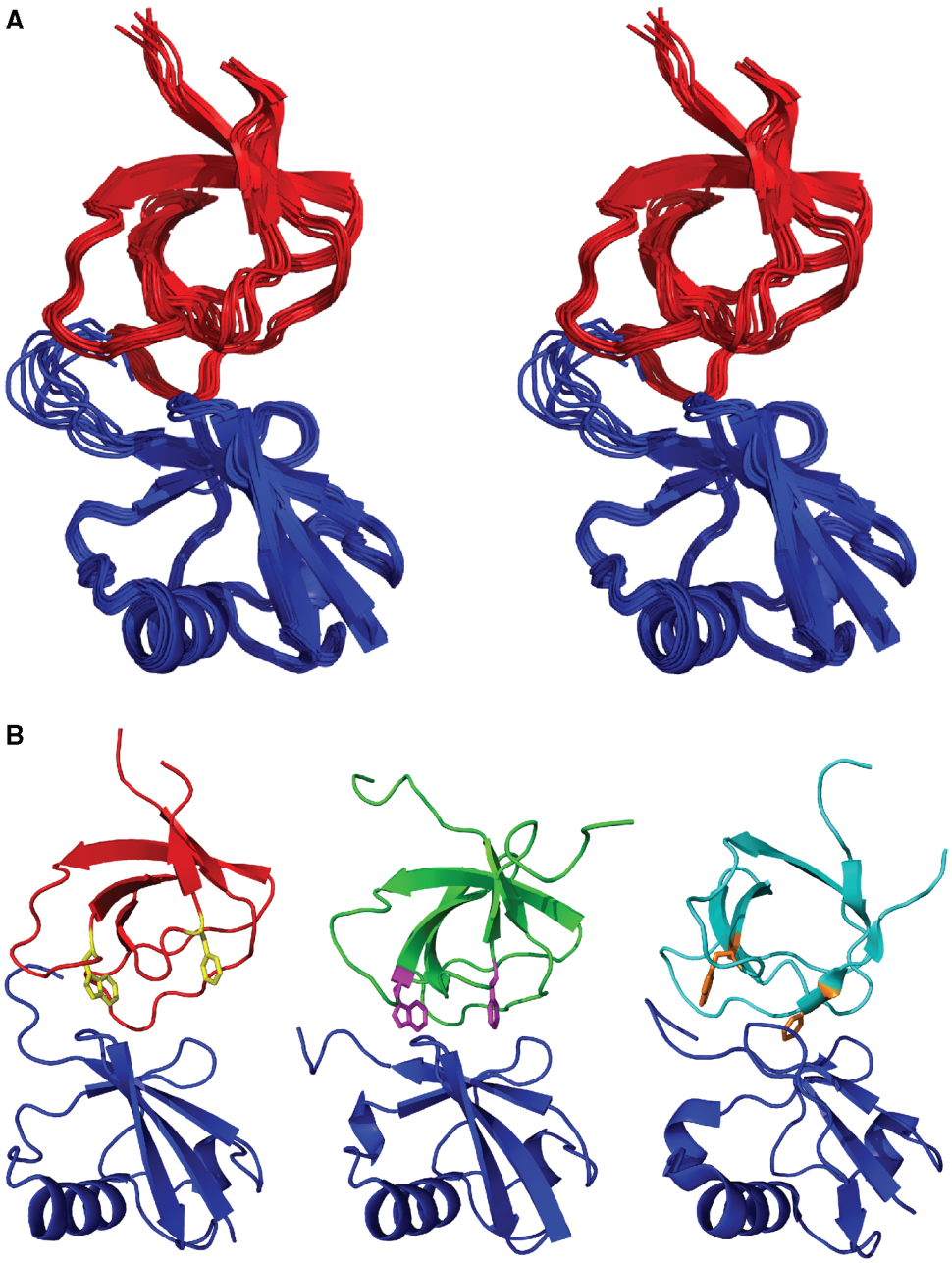


**Figure 5.** Structural model of the complex between CD2AP SH3-C and ubiquitin. (**A**) Stereo representation of the ensemble of 10 lowest-energy structures derived from the RDC titration protocol (SH3-C in red, ubiquitin in blue). (**B**) Comparison between the CD2AP SH3-C:Ubiquitin (SH3-C in red, ubiquitin in blue), Sla1 SH3-3:Ubiquitin complex (PDB entry 2JTA; SH3-3 in green, ubiquitin in blue) and CIN85 SH3-C:Ubiquitin (PDB entry 2K6D; SH3 in cyan, ubiquitin in blue). Trp43 and Phe59 in CD2AP SH3-C are shown in yellow sticks and the equivalent residues in Sla1 SH3-3 and CIN85 SH3-C are shown in magenta and orange sticks, respectively. The SH3:Ubiquitin complexes were superimposed on the backbone atoms of residues 4–71 of ubiquitin (RMSD of 0.74 and 1.32 Å for Sla1 and CIN85 to CD2AP, respectively).

best reproduced, are shown in Figure 6. The orientation of the partners very clearly changes, and is evidently incorrect even for complexes refined with data emanating from samples containing relatively high populations of complexed relative to free form. When the dissociation constant is sufficiently weak, it is therefore extremely risky to exploit RDC data sets from a single mixture even when the data are measured in the range of $0.7 < p_{\mathrm{bound}} < 1.0$, unless one can be certain of the exact population of free protein.

## Impact of RDC titration on the accuracy of molecular interfaces in weak complexes

Understanding the interaction structure of an organism's proteome is one of the key objectives of the many genomic and proteomic initiatives realized over recent decades. A complete understanding of molecular biology can only be derived from an atomic-level description of molecular interactions that control many cellular processes and are crucial for biological function. Weak molecular

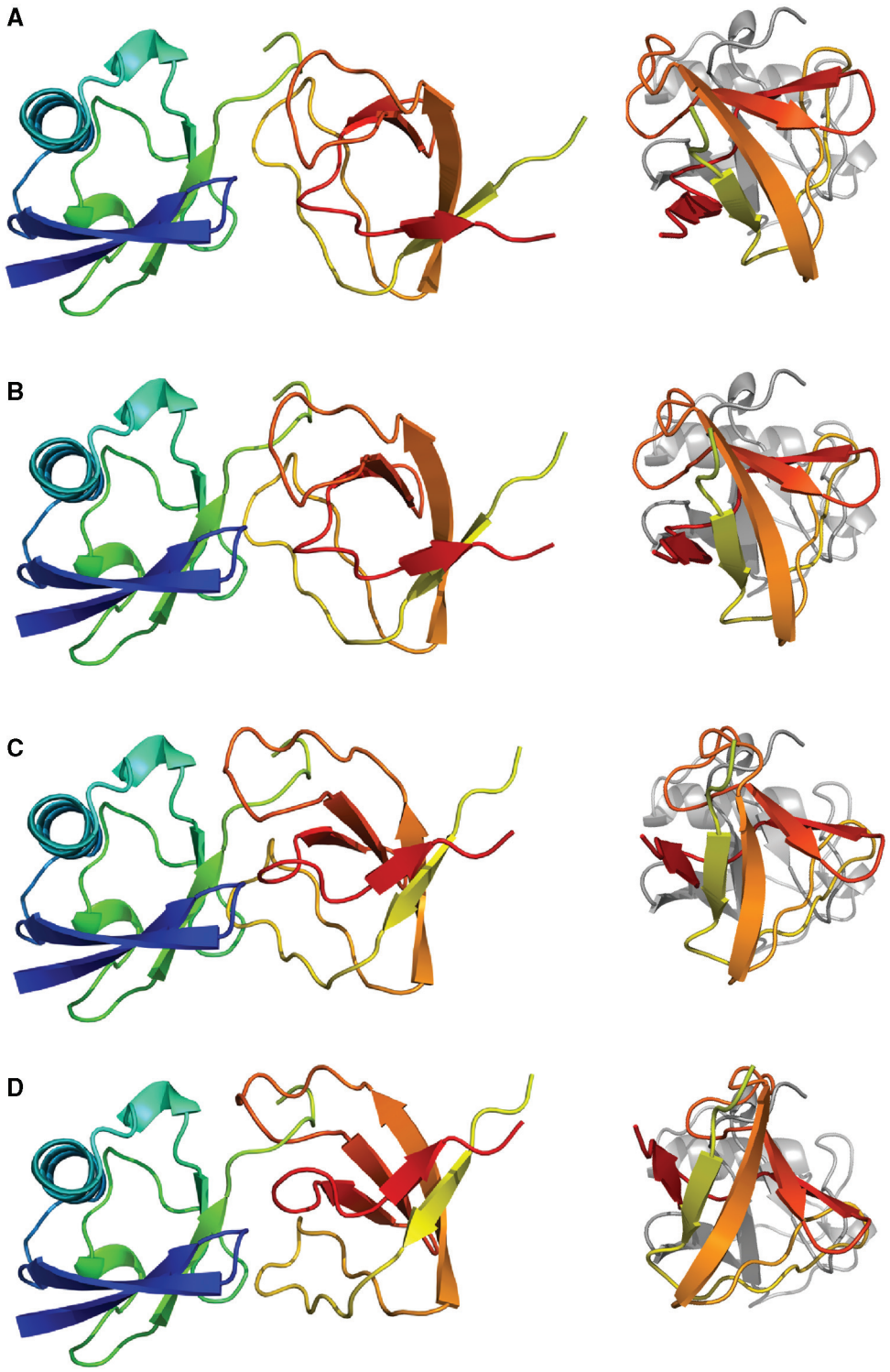


**Figure 6.** Effect of non-saturation on effective alignment and orientation of the SH3-Ubiquitin complex. Data were simulated from the bound and free states of ubiquitin and SH3 and mixed in ratios of 1.00:0.0 (**A**), 0.9:0.1 (**B**), 0.8:0.2 (**C**) and 0.7:0.3 (**D**). The relative orientation was determined by aligning the axes of the effective alignment tensors for the two domains. Right-hand panels represent a rotation of 90° about the vertical axis with respect to the left-hand panels. The ubiquitin domain is held fixed for the purposes of comparison in the figure. The alignment tensors for SH3 and Ubiquitin are respectively given by (A) $A_a = 12.2 \times 10^{-4}$, $A_r = 3.2 \times 10^{-4}$; $A_a = 13.3 \times 10^{-4}$, $A_r = 4.3 \times 10^{-4}$; (B) $A_a = 10.9 \times 10^{-4}$, $A_r = 2.3 \times 10^{-4}$; $A_a = 12.8 \times 10^{-4}$, $A_r = 4.0 \times 10^{-4}$; (C) $A_a = 10.0 \times 10^{-4}$, $A_r = 2.0 \times 10^{-4}$; $A_a = 12.4 \times 10^{-4}$, $A_r = 3.7 \times 10^{-4}$; (D) $A_a = 9.6 \times 10^{-4}$, $A_r = 3.0 \times 10^{-4}$; $A_a = 12.0 \times 10^{-4}$, $A_r = 3.4 \times 10^{-4}$. Differences in orientation relative to the fully bound form (A) can be measured by the differences in the Euler rotations of the alignment tensor axes for the two molecules: (B) $\delta\alpha = 10°$, $\delta\beta = 10°$, $\delta\gamma = 2°$; (C) $\delta\alpha = 32°$, $\delta\beta = 20°$, $\delta\gamma = 7°$; (D) $\delta\alpha = 54°$, $\delta\beta = 29°$, $\delta\gamma = 12°$.

interactions are important for a vast range of cellular events, such as transcription and replication, signal transduction, transient formation of encounter complexes and assembly of protein complexes. NMR spectroscopy is the technique of choice for studying weak protein–protein, protein–nucleic acid or nucleic acid–nucleic acid interactions, characterizing transiently populated molecular complexes at atomic resolution. RDCs are powerful constraints that can be used to describe intermolecular orientation, but great care needs to exercised when using these constraints for the study of weakly interacting proteins. In this study we demonstrate that even in the case of weakly populated free forms of either protein, incorrect orientational information can be aliased into inaccurate position of the proteins in the subsequently determined complex, a scenario that is not detectable from the raw RDC data. The importance of this observation should not be underestimated for the understanding of molecular interaction. The example described here clearly demonstrates that under experimental conditions where only 80% of the protein is in the complex, the relative orientation of the entire protein can be incorrectly determined, incurring errors of up to 40–50°. These errors cannot be detected, giving back-calculated restraints that are in perfect agreement with the data, unless the titration procedure introduced here is applied. The consequences of this source of error are important, potentially leading to completely erroneous interpretation of the physical forces controlling molecular association and dissociation, for example, electrostatic, hydrophobic or hydrogen bonding interactions, quite simply because the wrong amino acids will be aligned in the opposing interfaces.

## CONCLUSIONS

We have developed a robust approach to the exploitation of the unique orientational information available from RDCs in the case of weak interaction and rapid exchange between free and bound forms. We demonstrate that the measurement of RDC changes upon titration of one partner into the equilibrium mixture leads to accurate determination of bound forms for both partners that are otherwise experimentally unattainable. We further develop analytical methods that guarantee the robustness of the approach by accurately adjusting the effective level of alignment of bound and free forms at all titration points. The method is applicable to a large number of proteins that can be studied by classical chemical shift perturbation, as long as both proteins and complex can be successfully aligned in the same medium, and that the complex can also be aligned. This approach provides complementary conformational restraints to those available from intermolecular contact restraints within a reasonable experimental period (3–4 days). We expect that this technique will extend the already remarkable and unique ability of NMR to determine the binding modes of weak complexes and expect this approach to contribute further to our understanding of diverse interactomes and thereby the molecular basis of cellular processes in different organisms.

## SUPPLEMENTARY DATA

Supplementary Data are available at NAR Online.

## ACKNOWLEDGEMENTS

We thank Varian for providing double-labeled ubiquitin. 600 MHz spectra were recorded at Centre for Scientific Instrumentation (CIC) of the University of Granada and Institut de Biologie Structurale Grenoble. We thank Adrien Favier, Ewen Lescop and Rodolfo Rasia for pulse sequence development and spectrometer support.

## FUNDING

Grant BIO2005-04650 from the Spanish Ministry of Education and Science (MEC); the Commisariat à l'Energie Atomique; the French Centre National pour la Recherche Scientifique; the Université Joseph Fourier, Grenoble; the French Research Ministry through ANR NT05-4_42781 (to M.B.); ANR JCJC05-0077 (to B.B.); a return grant of the Junta de Andalucia (to A.I.A.); Lundbeckfonden and a long-term EMBO fellowship (to M.R.J.). J.L.O.R. and N.A.J.v.N. are recipients of an FPU and Ramón y Cajal research contract from the MEC, respectively; and the Access to Research Infrastructures activity in the 6th Framework Programme of the EC (Contract # RII3-026145, EU-NMR). Funding for open access charge: ANR NT05-4_42781.

*Conflict of interest statement*. None declared.

## REFERENCES

1. Chandonia,J.M. and Brenner,S.E. (2006) The impact of structural genomics: expectations and outcomes. *Science*, **311**, 347–351.
2. Levitt,M. (2007) Growth of novel protein structural data. *Proc. Natl. Acad. Sci. USA*, **104**, 3183–3188.
3. Kelly,W.P. and Stumpf,M.P.H. (2008) Protein–protein interactions, from global to local analyses. *Curr. Opin. Biotechnol.*, **19**, 396–403.
4. Devos,D. and Russell,R.B. (2007) A more complete, complexed and structured interactome. *Curr. Opin. Struct. Biol.*, **17**, 370–377.
5. Levy,E.D. and Pereira-Leal,J.B. (2008) Evolution and dynamics of protein interactions and networks. *Curr. Opin. Struct. Biol.*, **18**, 349–357.
6. Bader,S., Kühner,S. and Gavin,A.-C. (2008) Interaction networks for systems biology. *FEBS Lett.*, **582**, 1220–1224.
7. Nooren,I.M.A. and Thornton,J.M. (2003) Diversity of protein–protein interactions. *EMBO J.*, **22**, 3486–3492.
8. Vaynberg,J. and Qin,J. (2006) Weak protein–protein interactions as probed by NMR spectroscopy. *Trends Biotechnol.*, **24**, 22–27.
9. Tang,C., Iwahara,J. and Clore,G.M. (2006) Visualization of transient encounter complexes in protein-protein association. *Nature*, **444**, 383–386.
10. Takeuchi,K. and Wagner,G. (2006) NMR studies of protein interactions. *Curr. Opin. Struct. Biol.*, **16**, 109–117.
11. Tjandra,N. and Bax, (1997) A direct measurement of distances and angles in biomolecules by NMR in a dilute liquid crystalline medium. *Science*, **278**, 1111–1114.
12. Prestegard,J.H., Bougault,C.M. and Kishore,A.I. (2004) Residual dipolar couplings in structure determination of biomolecules. *Chem. Rev.*, **104**, 3519–3540.
13. Garrett,D.S., Seok,Y.-J., Peterkofsky,A., Gronenborn,A.M. and Clore,G.M. (1999) Solution structure of the 40,000 Mr phosphoryl transfer complex between the N-terminal domain of enzyme I and HPr. *Nat. Struct. Biol.*, **6**, 166–173.

14. Olejniczak,E.T., Meadows,R.P., Wang,H., Cai,M., Nettesheim,D.G. and Fesik,S.W. (1999) Improved NMR structures of protein/ligand complexes using residual dipolar couplings. *J. Am. Chem. Soc.*, **121**, 9249–9257.
15. Clore,G.M. (2000) Accurate and rapid docking of protein-protein complexes on the basis of intermolecular nuclear overhauser enhancement data and dipolar couplings by rigid body minimization. *Proc. Natl Acad. Sci. USA*, **97**, 9021–9026.
16. McCoy,M.A. and Wyss,D.F. (2002) Structures of protein–protein complexes are docked using only NMR restraints from residual dipolar coupling and chemical shift perturbations. *J. Am. Chem. Soc.*, **124**, 2104–2105.
17. Clore,G.M. and Schwieters,C.D. (2003) Docking of protein–protein complexes on the basis of highly ambiguous intermolecular distance restraints derived from 1H/15N chemical shift mapping and backbone 15N-1H residual dipolar couplings using conjoined rigid body/torsion angle dynamics. *J. Am. Chem. Soc.*, **125**, 2902–2912.
18. Bolon,P.J., Al-Hashimi,H.M. and Prestegard,J.H. (1999) Residual dipolar coupling derived orientational constraints on ligand geometry in a 53 kDa protein-ligand complex. *J. Mol. Biol.*, **293**, 107–115.
19. Koenig,B.W., Kontaxis,G., Mitchell,D.C., Louis,J.M., Litman,B.J. and Bax,A. Structure and orientation of a G protein fragment in the receptor bound state from residual dipolar couplings. *J. Mol. Biol.*, **322**, 441–461.
20. Jain,N.U., Noble,S. and Prestegard,J.H. (2002) Structural characterization of a mannose-binding protein–trimannoside complex using residual dipolar couplings. *J. Mol. Biol.*, **326**, 451–462.
21. Jain,N.U., Wyckoff,T.J.O., Raetz,C.R.H. and Prestegard,J.H. (2004) Rapid analysis of large protein–protein complexes using NMR-derived orientational constraints: the 95kDa complex of LpxA with acyl carrier protein. *J. Mol. Biol.*, **343**, 1379–1389.
22. Golovanov,A.P., Blankley,R.T., Avis,J.M. and Bermel,W. (2007) Isotopically discriminated NMR spectroscopy: a tool for investigating complex protein interactions in vitro. *J. Am. Chem. Soc.*, **129**, 6528–6535.
23. Ciechanover,A. (1998) The ubiquitin-proteasome pathway: on protein death and cell life. *EMBO J.*, **17**, 7151–7160.
24. Hicke,L., Schubert,H.L. and Hill,C.P. (2005) Ubiquitin-binding domains. *Nat. Rev. Mol. Cell Biol.*, **6**, 610.
25. Stamenova,S.D., French,M.E., He,Y., Francis,S.A., Kramer,Z.B. and Hicke,L. (2007) Ubiquitin binds to and regulates a subset of SH3 domains. *Mol. Cell*, **25**, 273–284.
26. He,Y., Hicke,L. and Radhakrishnan,I. (2007) Structural basis for ubiquitin recognition by SH3 domains. *J. Mol. Biol.*, **273**, 190–196.
27. Ortega Roldan,J.L., Ab,E., Romero Romero,M.L., Ora,A., Lopez Mayorga,O., Azuaga,A.I. and van Nuland,N.A.J. (2007) The high resolution NMR structure of the third SH3 domain of CD2AP. *J. Biomol. NMR*, **39**, 331–336.
28. Delaglio,F., Grzesiek,S., Vuister,G.W., Zhu,G., Pfeifer,J. and Bax,A. (1995) NMRPipe: a multidimensional spectral processing system based on UNIX pipes. *J. Biomol. NMR*, **6**, 277–293.
29. Johnson,B.A. and Blevins,R.A. (1994) NMRView – a computer-program for the visualization and analysis of NMR data. *J. Biomol. NMR*, **4**, 603–614.
30. Ruckert,M. and Otting,G. (2000) Alignment of biological macromolecules in novel nonionic liquid crystalline media for NMR experiments. *J. Am. Chem. Soc.*, **122**, 7793–7797.
31. Schanda,P., Van Melckebeke,H. and Brutscher,B. (2006) Speeding up three-dimensional protein NMR experiments to a few minutes. *J. Am. Chem. Soc.*, **128**, 9042–9043.
32. Lescop,E., Schanda,P. and Brutscher,B. (2007) A set of BEST triple-resonance experiments for time-optimized protein resonance assignment. *J. Magn. Reson.*, **187**, 163–169.
33. Goddard,T.D. and Kneller,D.G. (2003) *University of California*.
34. Brutscher,B. (2001) Accurate measurement of small spin-spin couplings in partially aligned molecules using a novel J-mismatch compensated spin-state-selection filter. *J. Magn. Reson.*, **151**, 332–338.
35. Hus,J.C., Marion,D. and Blackledge,M. (2000) De novo determination of protein structure by NMR using orientational and long-range order restraints. *J. Mol. Biol.*, **298**, 927–936.
36. Brunger,A.T., Adams,P.D., Clore,G.M., DeLano,W.L., Gros,P., Grosse-Kunstleve,R.W., Jiang,J., Kuszewski,J., Nilges,M., Pannu,N.S. *et al.* (1998) Crystallography and NMR system (CNS): a new software system for macromolecular structure determination. *Acta Cryst.*, **D54**, 905–921.
37. Dominguez,C., Boelens,R. and Bonvin,A.M.J.J. (2003) HADDOCK: a protein–protein docking approach based on biochemical or biophysical information. *J. Am. Chem. Soc.*, **125**, 1731–1737.
38. Sibille,N., Pardi,A., Simorre,J.P. and Blackledge,M. (2001) Refinement of local and long-range structural order in theophylline-binding RNA using $^{13}C$-$^{1}H$ residual dipolar couplings and restrained molecular dynamics. *J. Am. Chem. Soc.*, **123**, 12135–12146.
39. Sibille,N., Blackledge,M., Brutscher,B., Covès,J. and Bersch,B. (2005) Solution structure of the sulfite reductase flavodoxin-like domain from Escherichia coli. *Biochemistry*, **44**, 9086–9095.
40. Zuiderweg,E.R. (2002) Mapping protein–protein interactions in solution by NMR spectroscopy. *Biochemistry*, **41**, 1–7.
41. Bonvin,A.M.J.J. (2006) Flexible protein-protein docking. *Curr. Opin. Struct. Biol.*, **16**, 194–200.
42. Van Dijk,A.D.J. and Bonvin,A.M.J.J. (2006) Solvated docking, introducing water into the modelling of biomolecular complexes. *Bioinformatics*, **22**, 2340–2347.
43. Cornilescu,G., Marquardt,J.L., Ottiger,M. and Bax,A. (1998) Validation of protein structure from anisotropic carbonyl chemical shifts in a dilute liquid crystalline phase. *J. Am. Chem. Soc.*, **120**, 6836–6837.
44. Dosset,P., Hus,J.-C., Marion,D. and Blackledge,M. (2001) A novel interactive tool for rigid-body modeling of multi-domain macromolecules using residual dipolar couplings. *J. Biomol. NMR*, **20**, 223–231.
45. Zweckstetter,M. and Bax,A. (2002) Evaluation of uncertainty in alignment tensors obtained from dipolar couplings. *J. Biomol. NMR*, **23**, 127–1377.
46. Bernado,P. and Blackledge,M. (2004) Anisotropic small amplitude peptide plane dynamics in proteins from residual dipolar couplings. *J. Am. Chem. Soc.*, **126**, 4907–4920.
47. Bezsonova,I., Bruce,M.C., Wiesner,S., Lin,H., Rotin,D. and Forman-Kay,J.D. (2008) Interactions between the three CIN85 SH3 domains and ubiquitin: implications for CIN85 ubiquitination. *Biochemistry*, **47**, 8937–8949.
48. Korzhnev,D.M., Bezsonova,I., Lee,S., Chalikian,T.V. and Kay,L.E. Alternate binding modes for a ubiquitin–SH3 domain interaction studied by NMR spectroscopy. *J. Mol. Biol.*, **386**, 391–405.